

Mechanistic Basis for High Stereoselectivity and Broad Substrate Scope in the (salen)Co(III)-Catalyzed Hydrolytic Kinetic Resolution

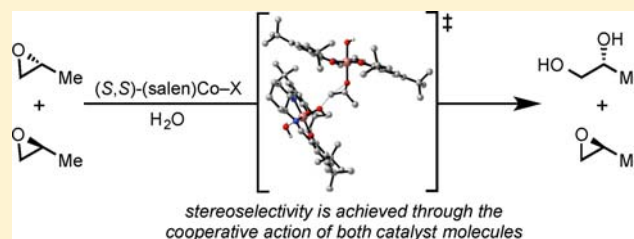
David D. Ford,[†] Lars P. C. Nielsen,[†] Stephan J. Zuend,[†] Charles B. Musgrave,[‡] and Eric N. Jacobsen^{*†}

[†]Department of Chemistry and Chemical Biology, Harvard University, Cambridge, Massachusetts 02138, United States

[‡]Department of Chemical and Biological Engineering, University of Colorado, Boulder, Colorado 80309, United States

S Supporting Information

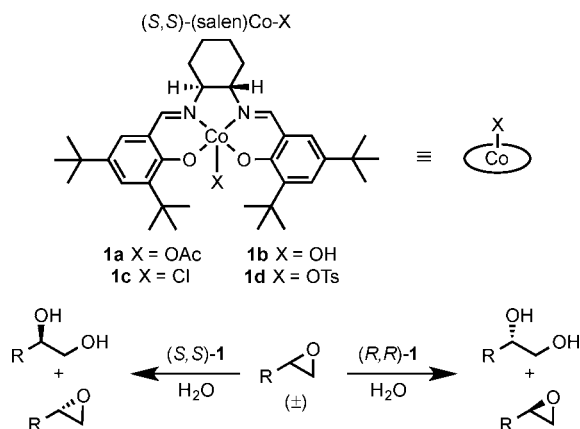
ABSTRACT: In the (salen)Co(III)-catalyzed hydrolytic kinetic resolution (HKR) of terminal epoxides, the rate- and stereoselectivity-determining epoxide ring-opening step occurs by a cooperative bimetallic mechanism with one Co(III) complex acting as a Lewis acid and another serving to deliver the hydroxide nucleophile. In this paper, we analyze the basis for the extraordinarily high stereoselectivity and broad substrate scope observed in the HKR. We demonstrate that the stereochemistry of each of the two (salen)Co(III) complexes in the rate-determining transition structure is important for productive catalysis: a measurable rate of hydrolysis occurs only if the absolute stereochemistry of each of these (salen)Co(III) complexes is the same. Experimental and computational studies provide strong evidence that stereochemical communication in the HKR is mediated by the stepped conformation of the salen ligand, and not the shape of the chiral diamine backbone of the ligand. A detailed computational analysis reveals that the epoxide binds the Lewis acidic Co(III) complex in a well-defined geometry imposed by stereoelectronic rather than steric effects. This insight serves as the basis of a complete stereochemical and transition structure model that sheds light on the reasons for the broad substrate generality of the HKR.



INTRODUCTION

The (salen)Co(III)-catalyzed hydrolytic kinetic resolution (HKR) is a powerful and widely used method for accessing enantiomerically pure terminal epoxides (Scheme 1).^{1,2} One of the most remarkable features of the HKR is the consistently high stereoselectivity obtained in the hydrolysis of a wide range of terminal epoxides, with the relative rate of reaction with the two enantiomers of the substrate (k_{rel}) >500 for some substrates and >100 for almost all examined.^{1b,3} Kinetic

Scheme 1. Hydrolytic Kinetic Resolution of Terminal Epoxides Catalyzed by (salen)Co(III) Complexes



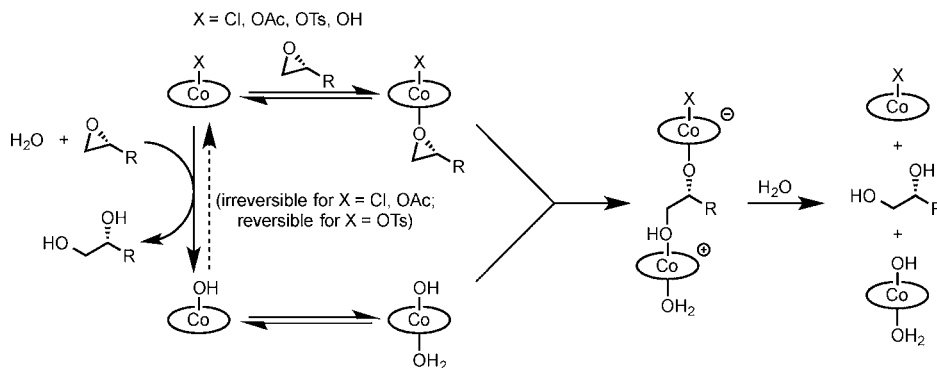
analyses of the HKR and related asymmetric ring-opening reactions have revealed a strict second-order rate dependence on the concentration of catalyst, indicating that two (salen)-Co(III) molecules are involved in the rate-limiting transition structure and thereby implicating a cooperative, bimetallic mechanism for epoxide ring-opening.^{4,5} Subsequent analyses of the HKR using a broad assortment of kinetic and structural probes have all led to a mechanistic picture wherein the rate- and stereoselectivity-determining step involves one Co(III) complex acting as a Lewis acid to activate the epoxide while another serves to activate water as a nucleophile via a (salen)Co-OH complex (Scheme 2).^{6,7} The rate of this step, and therefore of the overall reaction, depends strongly on the identity of the counterion in the (salen)Co-X precatalyst.^{6,8} In contrast, the stereoselectivity in the HKR was shown to be quite insensitive to counterion effects.⁶

While the mechanistic model in Scheme 2 presents a striking example of cooperativity in a catalytic reaction,⁹ it does not answer the fundamentally and practically significant question of why the HKR is so highly stereoselective while also so broad in substrate scope. In this paper, we analyze the stereoselectivity of the HKR using a combination of experimental and computational methods. We show that asymmetric induction in epoxide opening is imparted by both chiral complexes working cooperatively rather than by either complex alone. We provide

Received: August 2, 2013

Published: September 16, 2013

Scheme 2. Proposed Catalytic Mechanism for Epoxide Hydrolysis by (salen)Co(III) Complexes



evidence that stereochemical communication between the chiral complexes is mediated by the chiral, stepped conformation of the ligands. Finally, we advance a complete transition structure analysis for the epoxide ring-opening step in the HKR, wherein the relative geometries between the two (salen)Co(III) complexes in the epoxide ring-opening event account for the observed high stereoselectivity and broad substrate scope.

RESULTS AND DISCUSSION

1. Stereochemical Cooperativity in the HKR. A fundamental question underlying the mechanism of the HKR is whether stereoselectivity is controlled by the Lewis acidic complex that activates the epoxide, by the (salen)Co–OH complex that delivers the nucleophile, or in a coordinated manner by both complexes (Figure 1).¹⁰ Nonlinear-effect

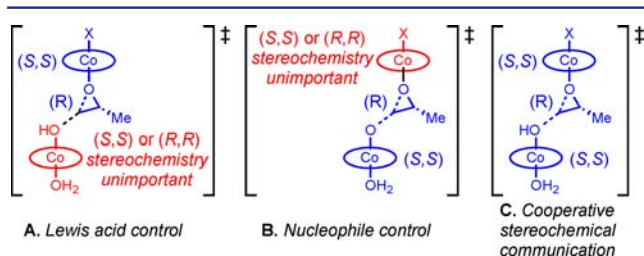


Figure 1. Limiting models for stereoinduction in the bimetallic epoxide ring-opening step. (A) The stereochemistry of the Lewis acidic complex determines stereoselectivity, with the stereochemistry of the nucleophile-delivery agent (salen)Co–OH being inconsequential. (B) The stereochemistry of the nucleophilic (salen)Co–OH complex controls stereoselectivity, with that of the Lewis acidic complex being unimportant. (C) High stereoselectivity is contingent on a matched relationship between the stereochemistry of both catalysts.

studies have been applied extensively in analyses of asymmetric catalytic reactions to probe whether interactions between chiral catalysts play any role in an asymmetric reaction of interest: a nonlinear dependence of product ee on catalyst ee may be ascribed to a stereochemically dependent interaction between catalysts, either in a resting state or in the stereoselectivity-determining transition state.¹¹ Interpretation of nonlinear effects in kinetic resolutions is inherently more challenging than in enantioselective reactions of prochiral substrates, because in a kinetic resolution, both product ee and starting material ee are conversion-dependent.¹² Nonetheless, Johnson and Singleton succeeded in evaluating nonlinear effects in the HKR by evaluating what they termed the differential kinetic

enantiomeric enhancement ($DKEE = (k_R - k_S)/(k_R + k_S)$) as a measure of stereoselectivity in kinetic resolutions. By plotting DKEE against the catalyst ee, they observed positive nonlinear effects in the (salen)Co(III)-catalyzed hydrolysis of terminal epoxides, thereby demonstrating that the (salen)Co complexes do indeed interact in a stereochemically dependent manner in the HKR.¹³ However, the mechanistic basis for this nonlinear effect has never been elucidated.^{12c}

In order to analyze the role of stereochemical cooperativity between (salen)Co(III) catalysts in the HKR, we sought to evaluate all eight stereochemically distinct bimetallic pathways that could lead to epoxide hydrolysis (Figure 2). Evaluation of

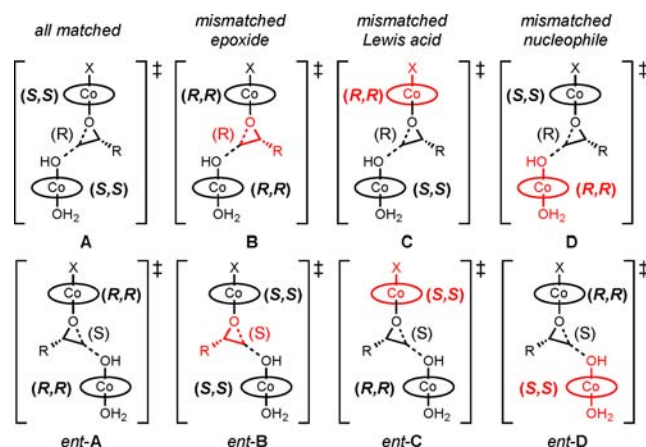


Figure 2. The eight possible stereochemically distinct pathways in a (salen)Co(III)-catalyzed hydrolysis of a terminal epoxide. In each case, the reaction component that is “mismatched” with respect to the other two components is shown in red.

the rate constants for each of these pathways would provide a direct measure of the importance of stereochemistry of each of the catalyst components in the HKR. Kinetic analysis of the HKR is complicated by the dynamic nature of catalyst partitioning between (salen)Co–X and (salen)Co–OH (Scheme 2), rendering the catalytic rate law a “moving target” that changes over the duration of the reaction.⁶ However, this complication is lifted if X = OH, that is, if the Lewis acid component in the HKR is the (salen)Co–OH complex 1b. This catalyst is more than 10-fold less reactive than more Lewis acidic complexes such as (salen)Co–OAc or (salen)Co–OTs.^{6a} However, as noted above, while the identity of the counterion X has a strong effect on the rate of epoxide hydrolysis, it has little effect on the stereoselectivity of the

HKR. Accordingly, analysis of the HKR using (salen)Co–OH complex **1b** alone allows straightforward rate studies uncomplicated by counterion effects, and can provide the same information about the basis of stereoselectivity as the more reactive (salen)Co–X derivatives. For these reasons, all analyses described in this study were carried out using complex **1b**.

The pathways in Figure 2 can be divided into four diastereomeric pathways with a given epoxide enantiomer (A–D), each of which has an equienergetic mirror-image counterpart (pathways *ent*-A–*ent*-D). Because the enantiomeric pathways are necessarily identical in energy, we can simplify the analysis by performing kinetic experiments with enantiopure epoxide, thereby limiting the number of possible pathways to four. The stereoselectivity in the kinetic resolution of any racemic terminal epoxide using enantiopure catalyst arises from the difference in rate between pathways A and *ent*-B (or the difference in rate between pathways *ent*-A and B). Since enantiomeric pathways are identical in rate, the difference in rate between pathways A and *ent*-B must be identical to the difference in rate between pathways A and B. As noted, the HKR is highly stereoselective ($k_{\text{rel}} > 100$) for almost all terminal epoxides examined to date, so from a kinetic standpoint pathway B is almost negligible relative to pathway A.

Pathways C and D each require a cooperative reaction between the opposite enantiomers of the catalyst. If either of these pathways can compete effectively with pathway A, then adding the mismatched enantiomer of **1b** to a reaction mixture containing enantiopure epoxide and matched catalyst would be expected to accelerate the rate of epoxide hydrolysis. Accordingly, the viability of pathways C and D was evaluated through kinetic experiments conducted with non-enantiopure mixtures of catalyst **1b**.

The rate of hydrolysis of (*R*)-1,2-epoxyhexane catalyzed by (*S,S*)-**1b** alone and with mixtures of (*S,S*)- and (*R,R*)-**1b** was determined by reaction calorimetry (Figure 3). As established previously, 1,2-epoxyhexane is a convenient substrate for kinetic studies of the HKR due to its relatively low volatility and favorable solubility properties, in addition to the fact that it

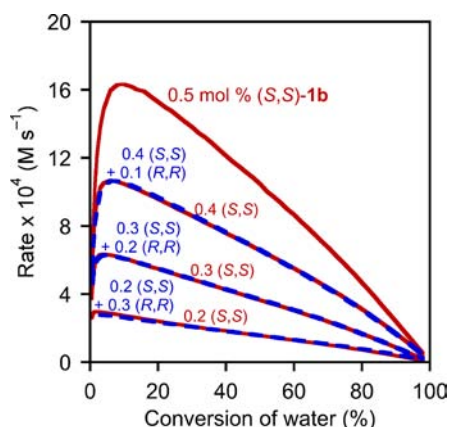


Figure 3. Dependence of the loading of matched catalyst (*S,S*)-**1b** and mismatched catalyst (*R,R*)-**1b** on the rate of hydrolysis of (*R*)-1,2-epoxyhexane ($[\text{epoxide}]_i = 6.6 \text{ M}$) in 1,2-hexanediol at 25 °C. The reaction rate is plotted as a function of conversion, with water ($[\text{H}_2\text{O}]_i = 2.8 \text{ M}$) as the limiting reagent. To generate the (salen)Co–OH complex **1b** quantitatively, the (salen)Co–Cl complex (*S,S*)-**1c** and/or (*R,R*)-**1c** (0.1–0.5 mol%) was added to the mixture of epoxide and diol and was aged for 60 min prior to addition of water.⁶

undergoes kinetic resolution with very high stereoselectivity ($k_{\text{rel}} > 300$ using either the (salen)Co–OAc precatalyst **1a** or the (salen)Co–OH catalyst **1b** generated *in situ*).^{1b} Comparison of the rates with enantiopure catalyst (solid red curves) and mixtures of catalyst enantiomers (dashed blue curves) reveals that the mismatched catalyst (*R,R*)-**1b** has no detectable effect on the rate of hydrolysis of (*R*)-1,2-epoxyhexane.

Therefore, there is no appreciable rate for epoxide hydrolysis involving two different enantiomers of catalyst working cooperatively (pathways C and D in Figure 2). For epoxide hydrolysis to occur, the absolute stereochemistry of both the nucleophilic and Lewis acidic (salen)Co(III) complexes must therefore be the same and be matched to the absolute stereochemistry of the epoxide (pathway A). As such, the question is resolved as to which of the two chiral (salen)Co(III) complexes is necessary for controlling the stereoselectivity in the HKR (Figure 1). The answer is that both are essential.¹⁴

2. The Salen Step as the Basis for Stereochemical Communication. While the experiments described above demonstrate that there is a strong stereochemical interaction between both molecules of (salen)Co(III) complex and the epoxide in the HKR ring-opening event, they do not answer the question of why stereoselectivity in the HKR is so high. Metal complexes of the salen ligand in **1** have been applied successfully in a wide range of asymmetric catalytic reactions,¹⁵ and understanding how this privileged ligand induces high enantioselectivity has been a topic of analysis for over two decades.^{16,17} One of the key insights to emerge from studies of certain other (salen)metal-catalyzed reactions is the importance of the stepped conformation of the salen ligand as a selectivity-determining element.^{18,19} The salen step is the result of a tilt of the salicylaldehyde aryl rings relative to the equatorial plane of the metal complex. This step is illustrated clearly in the (salen)Co(III) bis(aziridine) complex characterized by X-ray crystallography by Chin and co-workers (Figure 4).²⁰

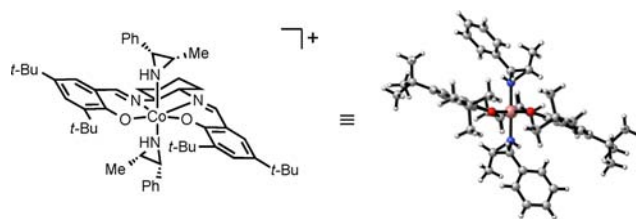


Figure 4. Chiral, stepped conformation of a cationic (salen)Co(III) bis(aziridine) complex. Figure generated from data retrieved from the Cambridge Structural Database, submission no. CCDC 185815, and ref 20. The counterions (a 1:1 mixture of chloride and acetate) and solvent (methylene chloride) are omitted for clarity.

The existence and absolute stereochemistry of the salen step are tied directly to the staggered conformation of the 1,2-diamine backbone in the ligand (Figure 5). The step itself possesses a chirality element, and by analogy to Fox's work with (salen)Ni(II) complexes,²¹ we use the helical chirality descriptors *P* and *M* to describe the absolute stereochemistry of the step in the salen structures (Figure 5). In the case of *trans*-1,2-diaminocyclohexane-derived salen ligands such as in **1**, the backbone is locked in a single, staggered chiral conformation, thereby setting the absolute stereochemistry of the helical chirality element in the salen step.²² In order to define the interactions responsible for high stereoselectivity in the HKR, we sought to probe whether it is the shape of the

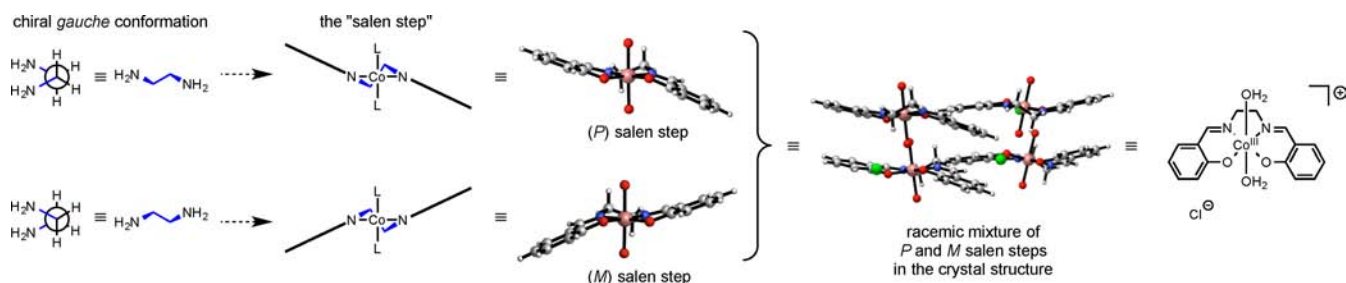
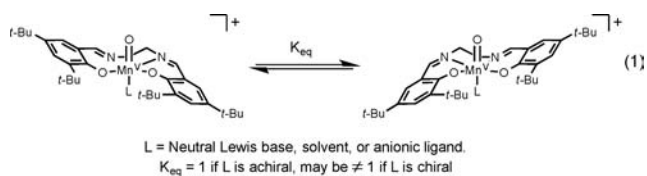


Figure 5. The salen step is an element of chirality in metal–salen complexes. The structure shown is derived from single-crystal X-ray diffraction data from ref 25. The structure on the right is the unit cell, containing two complexes of each enantiomeric conformer.

chiral diamine-derived backbone or the step chirality of the salen framework that plays the more dominant role. To accomplish this, we required a strategy to decouple these closely interconnected chirality elements.

The question of which chirality element of the salen ligand plays the more dominant role in stereoselection has been addressed in an elegant and compelling manner in the context of (salen)Mn(III)-catalyzed epoxidation reactions. Salen complexes derived from achiral 1,2-diamines such as 1,2-ethylenediamine can still adopt a chiral stepped conformation, but they exist as a racemic mixture of conformers (eq 1, $K_{\text{eq}} =$



1). In the presence of chiral additives such as amines, pyridine *N*-oxides, or BINOL-derived phosphates, these complexes have been shown to function as enantioselective epoxidation catalysts.²³

The chiral additives were assumed to bind directly to the metal center trans to the oxo ligand, so direct stereochemical communication from the chiral additive in the epoxidation event was considered unlikely. Instead, the catalysts have been

proposed to induce enantioselectivity by undergoing reaction selectively from one of the diastereomeric stepped conformers. The observation of high enantioselectivity in some cases with systems consisting of an achiral salen ligand with a chiral axial ligand has been taken as evidence that the salen step alone is sufficient for high stereoselectivity in (salen)Mn(III)-catalyzed epoxidation reactions.^{23c,d}

An analogous strategy of employing chiral axial ligands would not lend itself to a straightforward analysis of stereoselectivity in the HKR because of the complex ligand exchange phenomena and cooperative reactivity that are associated with this reaction (Scheme 2).^{6,10,24} Instead, we considered whether we might be able to apply a kinetic analysis of epoxide hydrolysis reactions catalyzed by achiral (salen)Co(III) complexes to shed light on the question of whether the salen step or the shape of the chiral diamine plays the principal role in stereoselection. This strategy was based on the fact that the salen step is a feature of (salen)Co(III) complexes regardless of whether the ligands are derived from chiral diamines. For example, the Co(III) complex of a 1,2-diaminoethane-derived salen ligand crystallizes as a racemic mixture of stepped chiral conformations (Figure 5).²⁵

Optimized, computed structures of neutral (salen)Co(III) complexes derived from both chiral and achiral 1,2-diamines are depicted in Figure 6. Each of these complexes is computed to be most stable in the low-spin, closed-shell configuration (see the Supporting Information). The similarity in the stepped structures of these complexes is particularly noteworthy, and

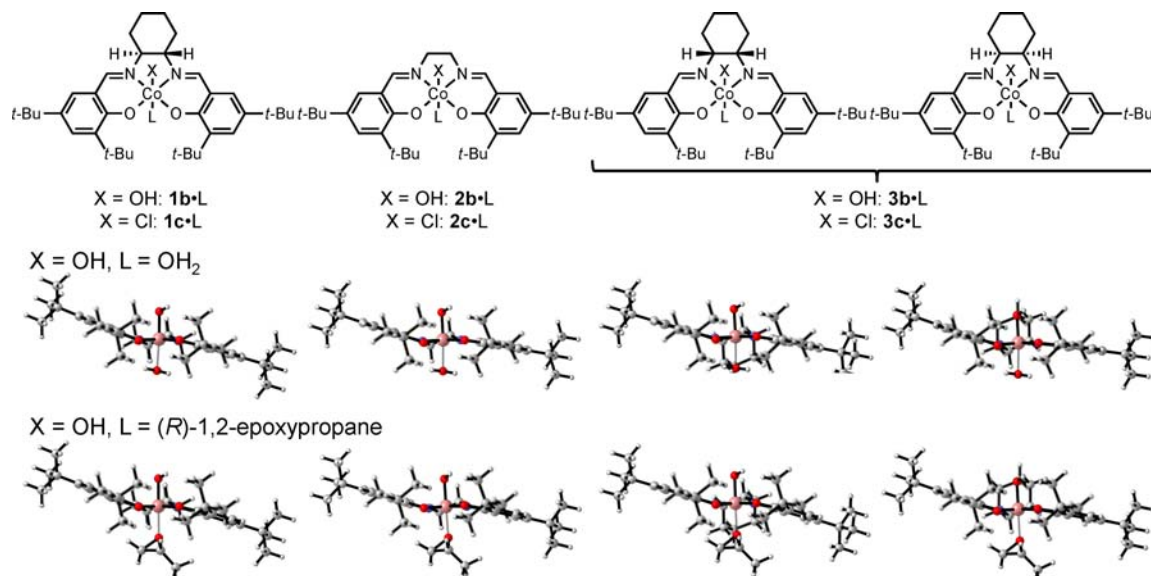


Figure 6. Optimized structures of neutral (salen)Co(III) complexes calculated as closed-shell singlets at the B3LYP/6-31G(d) level.

consistent with reported crystal structures of (salen)Co(III) complexes.^{26–28}

If the salen step alone were responsible for stereochemical communication between (salen)Co(III) complexes in the HKR, the different complexes depicted in Figure 6 with similar step structures but different backbone structures should participate comparably in cooperative catalysis either alone or with one another (Figure 7). We undertook a kinetic analysis of

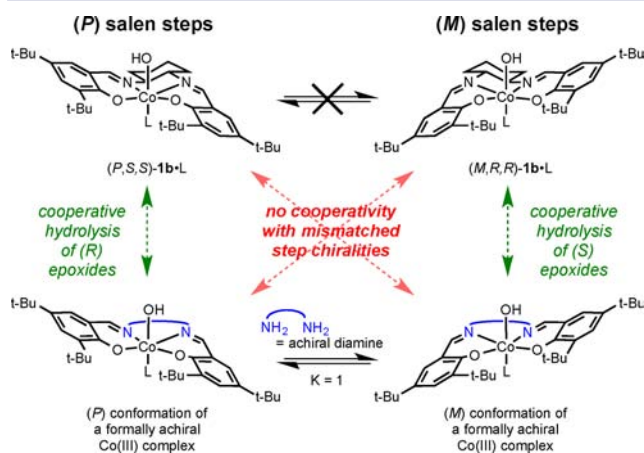


Figure 7. Summary of possible pathways for **1b** to engage in cooperative catalysis with a Co(III) complex of an achiral salen ligand. If the salen step mediates stereochemical communication, each (salen)Co(III) complex would only be able to undergo cooperative catalysis with another identical complex or with a different (salen)Co(III) complex of the same absolute step stereochemistry. L = H₂O or epoxide.

the achiral (salen)Co(III) complexes depicted in Figure 7 in epoxide hydrolysis reactions in order to determine whether this is the case.²⁹ The achiral (salen)Co–Cl complex derived from 1,2-diaminoethane (**2c**) is a competent catalyst, but was found to undergo significant deactivation during the course of epoxide hydrolysis reactions, thereby precluding a meaningful comparison of its rate to that of **1b**.

In contrast, the meso (salen)Co–Cl complex derived from *cis*-1,2-diaminocyclohexane (**3c**) was shown to be an effective and kinetically well-behaved precatalyst for the hydrolysis of 1,2-epoxyhexane. Previous kinetics studies have demonstrated that (salen)Co–Cl **1c** aged with epoxide is converted quantitatively to the corresponding hydroxo compound **1b** upon addition of water. The meso (salen)Co(III) analogue **3c** behaves in an identical manner, supporting the assumption that (salen)Co–OH **3b** is also generated quantitatively and is the active catalyst under these conditions. As we observed previously with compound **1b**, compound **3b** catalyzes hydrolysis of 1,2-epoxyhexane with a second-order dependence on the concentration of catalyst (Figure S1, Supporting Information). Given the similar kinetic behavior of **1b** and **3b**, we conclude that hydrolysis reactions catalyzed by Co(III) complexes **1b** and **3b** occur by analogous bimetallic mechanisms.

Having established that **3b** and **1b** have similar step but different diamine backbone structures (Figure 6), and that both catalyze epoxide hydrolysis by a second-order mechanism (Figure S2), we were in a position to address which chirality elements mediate stereochemical communication between (salen)Co(III) catalysts in the key epoxide ring-opening step. If (*P*)-**3b** were kinetically indistinguishable from (*P,S,S*)-**1b** and

(*M*)-**3b** were kinetically indistinguishable from (*M,R,R*)-**1b**, we would expect that hydrolysis of (*R*)-1,2-epoxyhexane catalyzed by (*P,S,S*)-**1b** (matched with respect to epoxide) would proceed at the same rate as a reaction catalyzed by twice the concentration of **3b** (which consists of 50% (*P*)-**3b**). The rates of these reactions were determined using reaction calorimetry, and indeed reactions carried out with **1b** or **3b** ($[(P,S,S)\text{-}1b] = [3b]/2$) proceed at very similar rates (Figure 8). The curves in

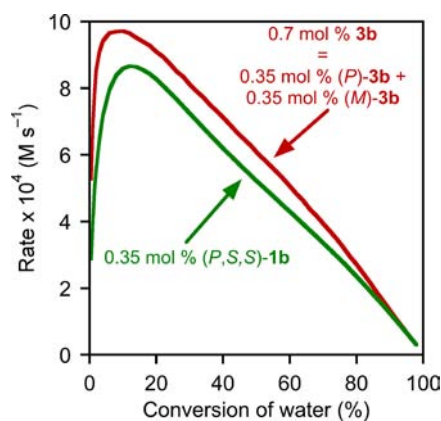


Figure 8. Comparison of rate of epoxide hydrolysis catalyzed by **3b** (0.7 mol %) and (*P,S,S*)-**1b** (0.35 mol %). The rates of hydrolysis of (*R*)-1,2-epoxyhexane ($[\text{epoxide}]_i = 6.0$ M) in 1,2-hexanediol at 25 °C as a function of conversion of water ($[\text{H}_2\text{O}]_i = 3.4$ M). In each experiment, **3c** or (*R,R*)-**1c** was added to the mixture of epoxide and diol and aged for 60 min, followed by water to generate **3b** or **1b**, respectively, *in situ*.

Figure 8 should overlay perfectly only if (*P,S,S*)-**1b** were kinetically indistinguishable from (*P*)-**3b** and if (*M*)-**3b** were completely incapable of promoting the hydrolysis of (*R*)-1,2-epoxyhexane (no catalysis through mechanisms analogous to pathways B, C, and D in Figure 2). The similarity of the kinetic behavior of catalysts **1b** and **3b** shown in Figure 8 is therefore taken as support for the hypothesis that the salen step plays the dominant role in mediating stereoselection in epoxide hydrolysis and that catalysis by **3b** occurs by a mechanism very similar to pathway A shown in Figure 2.³⁰

To further probe the question of the stereochemical requirements for **3b** to participate in catalysis, we assayed for cooperative reactivity between **3b** and **1b**. Hydrolysis of (*R*)-1,2-epoxyhexane catalyzed by mixtures of **3b** and (*M,R,R*)-**1b** (mismatched with respect to epoxide) was found to proceed at rates nearly identical to those of reactions catalyzed by **3b** alone (Figure 9).³¹ Hydrolysis of (*R*)-1,2-epoxyhexane catalyzed by mixtures of **3b** and the matched chiral catalyst, (*P,S,S*)-**1b**, provides a strikingly different result, with clear evidence of cooperativity between the two complexes (Figure 10).

The results of both experiments are consistent with the proposal that the stepped conformation of the salen ligand, rather than the shape of the chiral diamine backbone, is responsible for stereochemical induction in epoxide hydrolysis. In the experiment depicted in Figure 9, the observed epoxide hydrolysis can be attributed entirely to catalysis by the *P* conformer of **3b**, and no cooperative reactivity is observed with (*M,R,R*)-**1b** because the latter is mismatched with respect to the epoxide's absolute stereochemistry. In the experiment depicted in Figure 10, cooperative reactivity between **1b** and **3b** is observed, and this can be ascribed to the fact that the *P* conformer of **3b** and (*P,S,S*)-**1b** have the same step

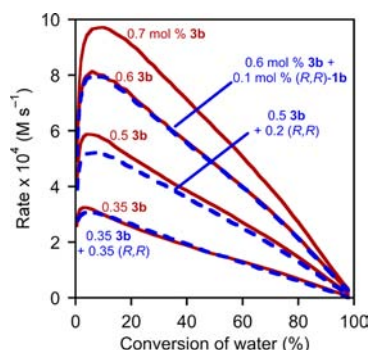


Figure 9. Rate dependence on amount of **3b** and (*R,R*)-**1b** catalyst. For each catalyst loading and/or mixture, we plot the rate of hydrolysis of (*R*)-1,2-epoxyhexane ($[\text{epoxide}]_i = 6.0 \text{ M}$) in 1,2-hexanediol at 25 °C versus conversion of water ($[\text{H}_2\text{O}]_i = 3.4 \text{ M}$). In each experiment, **3c** and/or (*R,R*)-**1c** (0.35–0.70 mol%) was added to the mixture of epoxide and diol and aged for 60 min, followed by water to generate **3b** or **1b**, respectively, in situ.

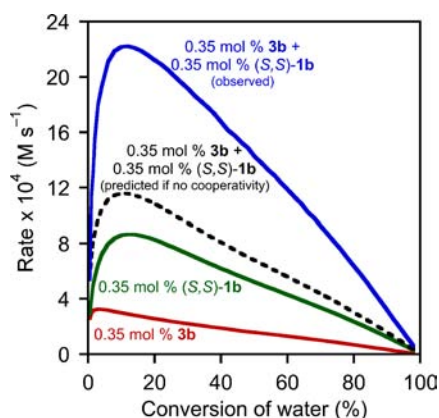


Figure 10. Rate dependence on amount of **3b** and (*P,S,S*)-**1b**. Plot of the rates of hydrolysis of (*R*)-1,2-epoxyhexane ($[\text{epoxide}]_i = 6.0 \text{ M}$) in 1,2-hexanediol at 25 °C versus conversion of water ($[\text{H}_2\text{O}]_i = 3.4 \text{ M}$) in 1,2-hexanediol. In each experiment, **3c** and/or (*S,S,S*)-**1c** (0.35 mol%) was added to the mixture of epoxide and diol and aged for 60 min, followed by water. The dotted black curve represents the rate of hydrolysis expected from the mixture of **3b** and (*P,S,S*)-**1b** if no cooperative catalysis between these two catalysts occurred.

stereochemistry, matched to that of the epoxide. Thus, catalysts with structurally different diamine backbones that still possess similar salen step features can operate cooperatively in epoxide hydrolysis only if the salen step absolute stereochemistries are matched, and matched to the stereochemistry of the epoxide. Such reactivity patterns would not be expected if the shape of the chiral diamine played an important role in recognition between catalysts in pathway A. We conclude that the salen step is the dominant factor mediating stereochemical communication in the HKR.

3. Computed Structure of (salen)Co(III)·Epoxide Complexes.

The experimental data described above provide strong evidence that stereoselectivity in the HKR is tied directly to the chiral, stepped nature of both (salen)Co(III) complexes in the epoxide ring-opening event. We turned to a computational analysis in order to glean a clearer understanding of how this stereochemical cooperativity leads to the remarkably high selectivity factors and broad substrate scope that are characteristic of the HKR. We chose the B3LYP density functional theory method,³² with a relatively small 6-31G(d) basis set, as the primary method due to the level of success with which it has been applied to other transition-metal-based systems.³³ Given the state of the art in high-performance computing hardware and electronic structure theory software, the choice of a relatively small basis set was critical to the feasibility of this analysis, as the ring-opening transition structures shown schematically in Figure 2 have ca. 700 electrons and 90 heavy atoms. Conscious of the well-documented limitations of B3LYP,³⁴ we repeated several key calculations at higher levels of theory, both with and without continuum solvent modeling.³⁵ The results obtained using these higher levels of theory were qualitatively similar to those found with B3LYP/6-31G(d) and support fully the conclusions drawn in this study. A summary of those analyses is provided in the Supporting Information.

As a first step in the computational analysis of the HKR, we sought to evaluate the geometries of epoxide complexation to the chiral (salen)Co(III) complex, and the extent to which these might depend on the absolute stereochemistry of the epoxide. In particular, the energetic cost of varying the O–Co–O–C dihedral angle θ in epoxide-(*S,S*)-**1b** complexes was evaluated systematically with (*R*)-1,2-epoxypropane (matched with respect to (*S,S*)-**1b**), (*S*)-1,2-epoxypropane (mismatched), and ethylene oxide (Figure 11).³⁶ This analysis reveals a strong

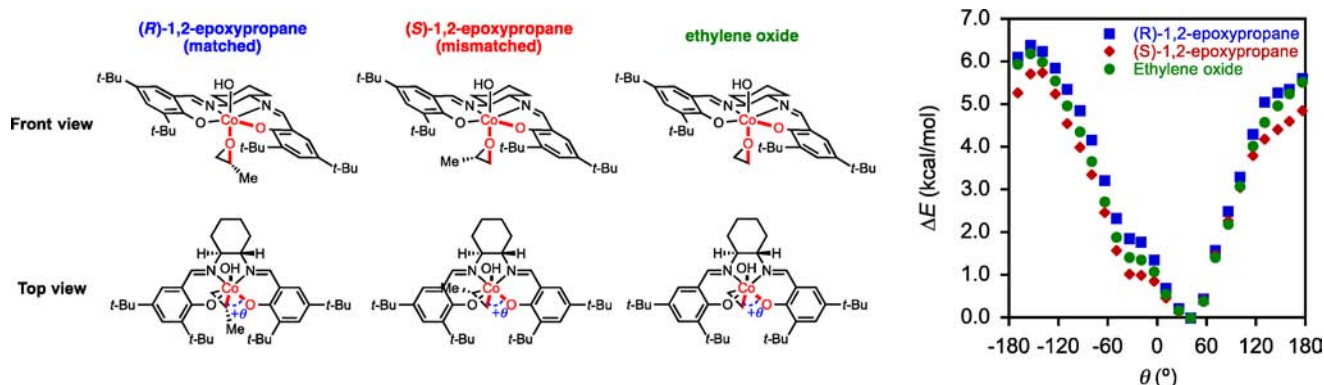


Figure 11. Plot of relative energy versus O–Co–O–C dihedral angle θ in a neutral (*S,S*)-(salen)Co(III) complex with bound (*R*)-1,2-epoxypropane (blue squares), (*S*)-1,2-epoxypropane (red diamonds), and ethylene oxide (green circles), calculated as closed-shell singlets at the B3LYP/6-31G(d) level. Each point represents the relative uncorrected electronic energy of an optimization performed with θ frozen and all other degrees of freedom permitted to relax. The minimum for each epoxide was set to $\Delta E = 0$ kcal/mol.

preference for epoxide binding within a narrow range of dihedral angles θ regardless of epoxide stereochemistry, with $\theta = 40^\circ$ as the global minimum for the three epoxides examined.³⁷

Comparison of the lowest energy computed structures of (S,S)-(salen)Co–OH with bound (R)- and (S)-1,2-epoxyhexane reveals only a 0.52 kcal/mol preference for binding of (R)-epoxypropane (Figure 12). This result is consistent with

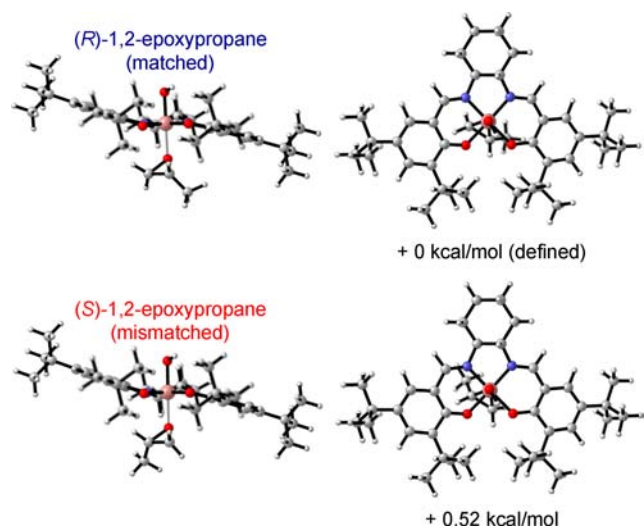


Figure 12. Structures of neutral (S,S)-(salen)Co–OH complexes with bound (R)-1,2-epoxypropane and (S)-1,2-epoxypropane, calculated as closed-shell singlets at the B3LYP/6-31G(d) level.

kinetic analyses of HKR reactions^{6a} and binding studies performed using ¹H NMR,³⁸ which showed that both enantiomers of epoxide bind rapidly and reversibly to chiral (salen)Co(III) complexes such as **1b**, and with approximately equal affinity. Taken together, the experimental and computational data reveal that that epoxides are bound in a well-defined orientation with respect to the (salen)Co(III) complex independent of the stereochemistry of the epoxide, but that differential epoxide complexation is not responsible for stereoselectivity in the HKR.

4. Computational Characterization of the Nucleophilic (salen)Co–OH Complex. Together with the epoxide complex analyzed in section 3, the other critical reacting partner in the HKR is the nucleophilic (salen)Co–OH complex, so we also sought to characterize this intermediate computationally. In particular, we were interested in defining the coordination geometry and spin state of the most reactive (salen)Co–OH complex. A hexacoordinate, low-spin (salen)Co(OH₂)(OH) complex (**¹1b**·H₂O, *S* = 0)³⁹ has been implicated as the reactive nucleophilic species in the HKR on the basis of kinetic analyses.⁶ These species have been shown to be nucleophilic: hexacoordinate Co(III) hydroxo complexes studied as metalloprotease mimics are competent nucleophiles in the hydrolysis of pendant ester groups of *N*-coordinated amino ester ligands.⁴⁰

Recently, an alternative, pentacoordinate, intermediate-spin (salen)Co–OH complex (**³1b**, *S* = 1) was proposed in a separate study as a potentially reactive species on the basis of the assignment of **³1c** ((salen)Co–Cl) in CH₂Cl₂ solution by magnetic susceptibility measurements.³⁸ In this analysis, the authors found that in donor solvents such as THF, there is an equilibrium between diamagnetic and paramagnetic species. This led us to consider whether **³1b** and **¹1b**·H₂O might both

be accessible under the conditions of the HKR reaction and, if so, which of those is the active nucleophile in the epoxide ring-opening. On the basis of a superficial analysis, the triplet **³1b** might be expected to be more reactive, as low-spin, octahedral d⁶ complexes such as **¹1b**·H₂O are typically inert to ligand substitution reactions.⁴¹

Optimized, computed structures of **¹1b**·H₂O and **³1b** are presented in Figure 13.⁴² Six-coordinate **¹1b**·H₂O adopts a



Figure 13. Structures of potential nucleophilic catalysts **³1b** and **¹1b**·H₂O optimized at the B3LYP/6-31G(d) level of theory.

pseudo-octahedral geometry with a distinct step conformation as discussed in section 2, whereas five-coordinate **³1b** adopts a distorted square pyramidal geometry.⁴³ The calculations predict that **³1b** is stable as a five-coordinate complex and has very little affinity for water, while **¹1b**·H₂O is most stable as a six-coordinate complex and therefore binds water tightly. Whereas different levels of theory provided subtly different results, the general picture that emerges is that the lowest energy five-coordinate complexes are triplets, while the lowest energy six-coordinate complexes are singlets.⁴⁴ After examining individual Co(III) complexes in the ground state, we extended our analysis of spin state to the bimetallic epoxide ring-opening transition structures (Figure 14).

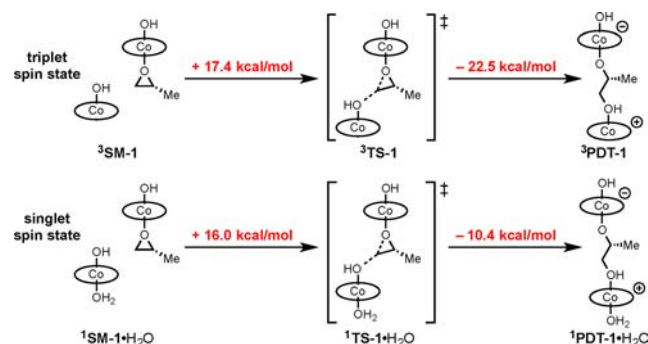


Figure 14. Relative reactivity of the singlet and triplet nucleophiles in the epoxide ring-opening transition structure for (salen)Co–OH at the B3LYP/6-31G(d) level in the gas phase. Structures in the singlet spin state were calculated as closed-shell configurations. Energies are reported as the difference in uncorrected electronic energy.

In a comparison of the calculated barriers to ring-opening transition structures of 1,2-epoxypropane (TS-1), we found that **¹1b**·H₂O is in fact more nucleophilic than **³1b**: the barrier for epoxide opening in the singlet manifold is 1.4 kcal/mol lower than what is calculated for the triplet manifold (Figure 14).^{45,46} These calculations demonstrate that the hydroxo ligand in this six-coordinate Co(III) complex **¹1b**·H₂O is in fact highly nucleophilic.

Analysis of the computed transition structures (Table 1) provides a potential explanation: the epoxide ring-opening transition state comes early on the reaction coordinate, with the

Table 1. Key Bond Lengths (Å) on the Reaction Coordinate from **1b** to PDT-1 for the Singlet and Triplet Spin States

bond	³ 1b	¹ 1b · H ₂ O	¹ 1b · E _{mat}	¹ TS-1 · H ₂ O	³ TS-1	¹ PDT-1 · H ₂ O	³ PDT-1
a	1.82	1.82	—	1.86	1.91	1.92	2.35
b	—	—	—	1.97	1.96	1.49	1.44
c	—	—	1.45	1.88	1.90	2.30	2.35
d	—	—	2.09	1.98	1.97	1.94	1.83

hydroxo ligand still fully associated to the Co(III) center. As such, nucleophilicity is not tied to the coordinative stability or lability of the hydroxo ligand, but rather to its nucleophilicity when bound to cobalt. We note the possibility that crossover to the triplet manifold plays a role in achieving catalyst turnover after the rate-determining epoxide ring-opening step. On the basis of this analysis and the previously reported kinetic analysis, we conclude that ¹**1b**·H₂O is indeed the nucleophilic partner in the HKR, and we use this structure in the remainder of the calculations in this paper.

5. Cooperative Stereochemical Communication in Epoxide Ring-Opening. Having elucidated the most salient features of the structure of both the (salen)Co–epoxide complex and the reactive (salen)Co–OH complex that participate in the HKR reaction, we sought to establish how these catalysts achieve stereoselectivity in the epoxide ring-opening reaction. The experimental results described in section 1 demonstrate that a stereochemical match is required between the epoxide and the two molecules of (salen)Co(III) in the epoxide ring-opening reaction, and determining whether this requirement could be reproduced computationally was a logical starting point for our analysis. Specifically, we sought to compare the calculated transition structure energies of the “all-matched” **TS-1**·H₂O with diastereomeric transition structures corresponding to pathways *ent*-B, C, and D introduced in Figure 2.

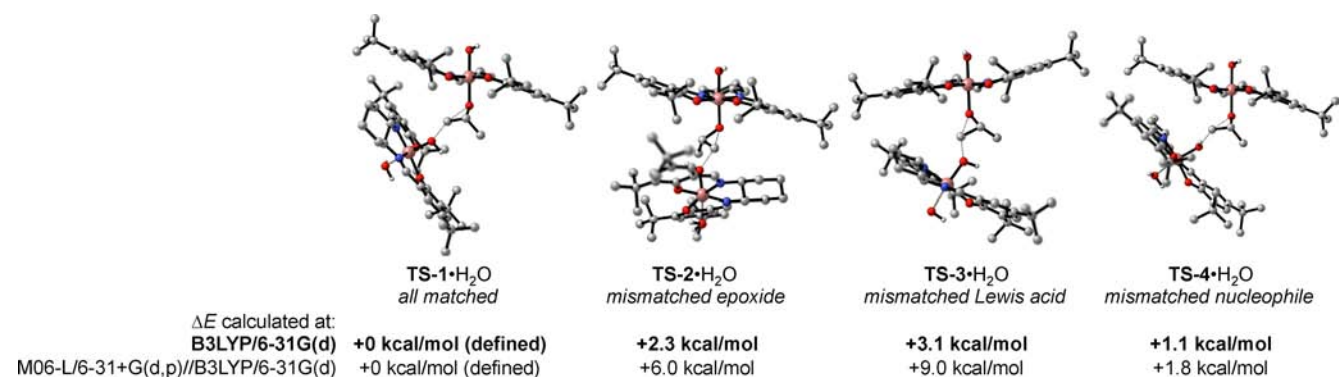
To more effectively model dispersive interactions that the B3LYP functional tends to underestimate, single-point calculations were performed on the B3LYP-optimized geo-

metries using Truhlar’s M06-L meta-GGA functional and the larger 6-31+G(d,p) basis set, which performs well in benchmarks for a range of noncovalent interactions.⁴⁷ The related Minnesota functional M05-2X has been shown to accurately predict catalyst structure–enantioselectivity relationships in reactions that are dominated by noncovalent interactions, although this method sometimes overestimates the magnitude of these selectivity trends.⁴⁸ Calculations with both the B3LYP and M06-L methods described above show that changing the absolute stereochemistry of either molecule of (salen)Co(III) catalyst or the epoxide resulted in a significantly higher transition structure energy (Figure 15). These data show that the stereochemical match required in HKR reactions is reproduced remarkably well with the chosen DFT methods.

Comparison of **TS-1**·H₂O and **TS-2**·H₂O is of particular interest, because the difference in energy between these two transition structures corresponds to the stereoselectivity of the kinetic resolution of a racemic epoxide with enantiopure catalyst (i.e., the HKR reaction). Inspection of **TS-2**·H₂O reveals that the nearest contact between the two (salen)Co(III) complexes is between the *tert*-butyl group at the salicylidene 5-position of the Lewis acidic complex and the backbone cyclohexane ring on the nucleophile-delivering catalyst (Table 2). Superficially, invoking such a contact as playing a role in

Table 2. Diastereomeric Transition Structures for Epoxide Opening

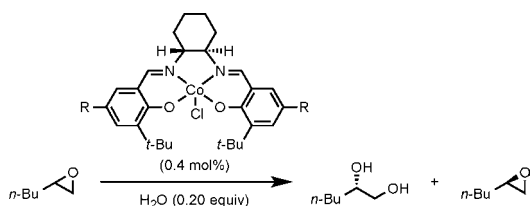
	TS-1 ·H ₂ O	TS-2 ·H ₂ O	TS-3 ·H ₂ O	TS-4 ·H ₂ O
Lewis acid	(<i>S,S</i>)	(<i>S,S</i>)	(<i>R,R</i>)	(<i>S,S</i>)
epoxide	(<i>R</i>)	(<i>S</i>)	(<i>R</i>)	(<i>R</i>)
nucleophile	(<i>S,S</i>)	(<i>S,S</i>)	(<i>S,S</i>)	(<i>R,R</i>)
bond a (Å)	1.86	1.86	1.86	1.86
bond b (Å)	1.97	1.95	1.98	1.96
bond c (Å)	1.88	1.89	1.89	1.88
bond d (Å)	1.98	1.98	1.99	1.98
angle θ (deg)	54.4	51.8	8.3	44.8

**Figure 15.** Epoxide ring-opening transition structures optimized at the B3LYP/6-31G(d) level of theory, presented along with the difference in energy between each structure and **TS-1**·H₂O. The selectivity was also calculated from single-point energies at the M06-L/6-31+G(d,p) level of theory with the B3LYP/6-31G(d) geometry. C–H bonds are omitted for clarity.

stereoiduction seems to be inconsistent with the results presented in section 2, which showed that the salen step mediates the stereochemical match between catalysts, and that the shape of the backbone plays a less significant role. The precise interpretation of the kinetics experiments in section 2 is more subtle, however: the data only show that the “all-matched” pathway A proceeds at comparable rates for **1b** and **3b** (Figure 8) and that other pathways are too slow to detect by reaction calorimetry. The data are not sufficient to conclude whether the interactions that destabilize pathways B–D for **1b** are the same as those that destabilize the analogous pathways for **3b**.

To test the effect of ligand bulk at the salicylidene 5-position experimentally, we prepared a series of substituted catalysts and determined each catalyst's stereoselectivity in (\pm)-1,2-epoxyhexane hydrolysis (Table 3).⁴⁹ The data reveal that the size of

Table 3. Selectivity Factors in Epoxide Hydrolysis with Substituted Catalysts



entry	R	selectivity factor ^a
1	H	62 ± 5
2	Me	82.14 ± 0.04
3	Et	146.5 ± 0.4
4	<i>i</i> -Pr	368 ± 1
5	<i>t</i> -Bu	620 ± 40
6	SiMe ₃	524 ± 9

^aAverage of two independent experiments ± 1 standard deviation. Determined by GC analysis of acetylated 1,2-hexanediol isolated from the reaction mixture.

the substituent indeed has a significant effect on stereoselectivity of epoxide hydrolysis, with larger substituents generally resulting in more selective catalysts.^{50–53} These results are supported by computational analysis with the M06-L functional (Supporting Information), which predicts that the transition state leading to hydrolysis of the mismatched enantiomer of epoxide must distort to accommodate the more sterically demanding 5,5' substituents, and that this distortion is costly in energy and therefore leads to enhanced stereoselectivity.

6. Intrinsic Stereoselectivity of (salen)Co–OH as a Lewis Acid for Epoxide Activation. As demonstrated above, DFT calculations of HKR transition structures provided good agreement with experimental stereoselectivities and even served to uncover a specific steric interaction that is important for selectivity. Our resulting confidence in the utility of these calculations prompted us to consider addressing questions related to the HKR computationally that are not readily addressable experimentally. These include the intrinsic stereoselectivity of (salen)Co–OH complex **1b** both as a Lewis acid for epoxide activation and as a nucleophile-delivery agent.

As established in section 1, a stereochemical match between the two (salen)Co(III) complexes is necessary for epoxide ring-opening to occur. However, the question remains unanswered as to whether the Lewis acid complex alone is capable of

inducing high stereoselectivity in epoxide ring-opening. As illustrated in Figure 16, both enantiomers of epoxide bind to

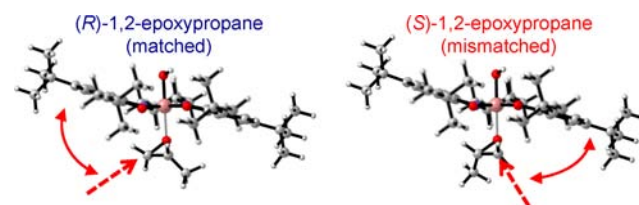


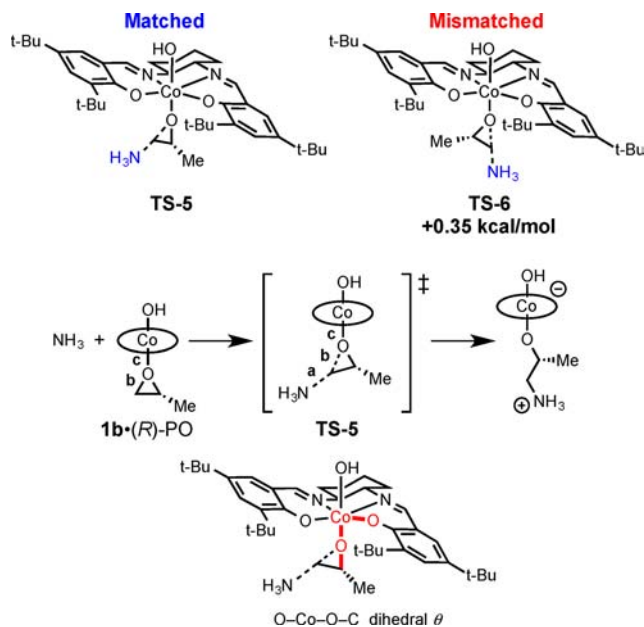
Figure 16. Whereas the epoxide ring is held in the same orientation with respect to the catalyst for both enantiomers of epoxide, an incoming nucleophile attacking the less substituted epoxide carbon is expected to experience different steric interactions with the stepped conformation of the catalyst, depending on the stereochemistry of the epoxide (red arrows).

the (salen)Co(III) complex in the same orientation with respect to the salen step. As such, approaching nucleophiles attacking the less substituted carbon of the epoxide experience different steric interactions with the Lewis acid catalyst depending on the stereochemistry of the epoxide.

As discussed in section 1, it is impossible to isolate the two roles of the (salen)Co(III) complex—epoxide activation and nucleophile delivery—experimentally because of the rapid ligand exchange that is characteristic of this system.¹⁰ On the other hand, computational analysis is well suited to address this question because the composition of the calculated structure can be controlled precisely. To evaluate whether (salen)Co–OH could be a highly stereoselective Lewis acid in the absence of a chiral nucleophile-delivery agent, we investigated the hypothetical reaction of ammonia with epoxides activated by (salen)Co–OH. We chose ammonia for its lack of charge, its small size, and its symmetry about the forming C–N bond—all desirable properties for a straightforward computational investigation. The results demonstrate that the Lewis acidic (salen)Co(III) catalyst alone does not activate epoxide stereoselectively: the calculated stereoselectivity of 0.35 kcal/mol for 1,2-epoxypropane actually represents an erosion of selectivity from the calculated ground-state preference of 0.52 kcal/mol for binding the matched enantiomer of epoxide (Table 4).

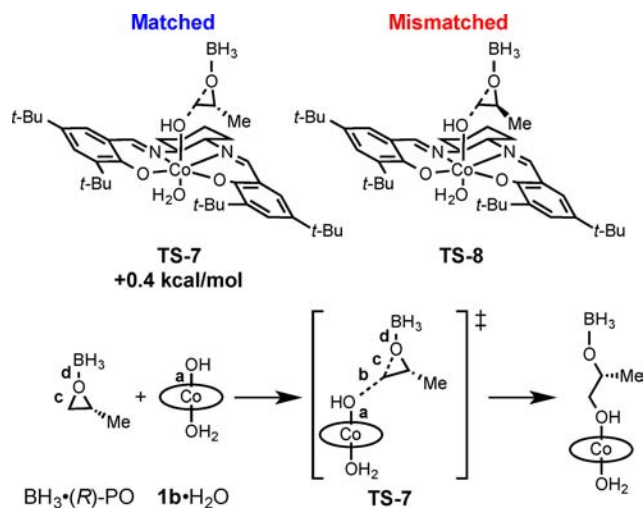
7. Intrinsic Stereoselectivity of (salen)Co(OH)(OH₂) as a Nucleophile. Having established that the calculated selectivity in our DFT model does not arise from (salen)Co–OH selectively activating the matched enantiomer of epoxide for attack, we set out to address the alternative possibility that (salen)Co(OH)(OH₂) (**1b**·H₂O) alone might be a highly stereoselective nucleophile-delivering agent that can discriminate between enantiomers of epoxide. If this were so, **1b**·H₂O should be able to discriminate between two enantiomers of an epoxide bound to an achiral Lewis acid. We selected borane as the Lewis acid for computational analysis of this hypothetical reaction for reasons analogous to those that led us to choose ammonia as our test nucleophile: borane is small, neutral, and symmetrical. However, this analysis is considerably more nuanced than the reaction of **1b**·(epoxide) with ammonia, as the nucleophilic oxygen atom of **1b**·H₂O might be reactive in a variety of trajectories. After thoroughly examining possible trajectories for nucleophilic addition to epoxide, we determined that in the lowest energy pathway there is actually a slightly lower barrier to opening the “mismatched” enantiomer of epoxide (Table 5). The analyses in this and the

Table 4. Transition Structures for the Hypothetical Reaction of Ammonia with Epoxides Activated by (S,S)-(salen)Co–OH



	1b-(R)-PO	1b-(S)-PO	TS-5	TS-6
bond a (Å)	–	–	2.00	2.00
bond b (Å)	1.45	1.45	1.94	1.93
bond c (Å)	2.09	2.09	1.99	2.00
angle θ (deg)	40.5	40.2	48.9	42.6

Table 5. Transition Structures for the Hypothetical Reaction of (S,S)-(salen)Co–OH with Borane-Activated 1,2-Epoxypropane



	1b-H ₂ O	BH ₃ -(R)-PO	TS-7	TS-8
bond a (Å)	1.82	–	1.86	1.86
bond b (Å)	–	–	2.03	2.02
bond c (Å)	–	1.46	1.84	1.83
bond d (Å)	–	1.67	1.57	1.57

preceding sections allow us to conclude that neither (salen)Co complex alone is responsible for the high stereoselectivity in the HKR, and that instead catalyst–catalyst interactions must be responsible. The remainder of this article endeavors to elucidate the precise basis for this remarkable cooperative effect.

8. Stereochemical Model for the HKR. As noted in the Introduction, consistently high stereoselectivities are obtained in (salen)Co(III)-catalyzed kinetic resolutions of terminal epoxides. For this reason, any meaningful stereochemical model for the HKR should shed light on why the steric properties of the epoxide substituent have so little impact on the stereoselectivity of the ring-opening reaction.

A visual inspection of the lowest energy transition structure, TS-1·H₂O (Figure 15), suggests a possible explanation: the epoxide substituent (in this case, methyl), which is the element that can be varied without negative impact on reaction stereoselectivity, projects into a large open space between the two Co(III) complexes. We evaluated whether this is the case in the HKR of a variety of different epoxides by optimizing matched epoxide-opening transition structures analogous to TS-1·H₂O and mismatched transition structures analogous to TS-2·H₂O for epoxides with different steric and electronic properties. Each of the epoxides subjected to this analysis undergoes hydrolysis with high stereoselectivity under (salen)-Co(III) catalysis.

Both “matched” and “mismatched” transition structure geometries remain remarkably unchanged upon changing the epoxide substituent in TS-1·H₂O from methyl to *tert*-butyl, cyclohexyl, or phenyl (Figure 17).⁵⁴ These structures give a striking perspective on a molecular assembly that is at once highly selective in epoxide kinetic resolution and remarkably promiscuous in accommodating a broad range of terminal epoxides: the epoxide substituent does not participate in any significant interactions in the stereoselectivity-determining transition structure; rather, its primary role is only to determine the position of the more reactive, less substituted position of the epoxide with respect to the chiral salen ligand.

We conclude that stereoselectivity in the HKR of terminal epoxides arises primarily from the catalyst–catalyst interactions taking place in the different transition structures, and not from specific interactions with the epoxide enantiomers. If this model is correct, one could imagine that the chiral (salen)Co(III) catalysts should exert a form of stereoselectivity even with ethylene oxide, which is achiral and bears no epoxide substituent at all. In that case, stereoselectivity would be manifested as a preference for addition to one electrophilic position over the other. While this prediction would be extremely difficult to test experimentally—the product in each case is simply ethylene glycol—it can be addressed quite readily using computational tools.

We replaced the epoxide methyl substituent in TS-1·H₂O and TS-2·H₂O with a hydrogen atom and fully optimized the resulting structure to a transition structure (Figure 18). These structures overlay nearly perfectly with TS-1·H₂O and TS-2·H₂O, and there is a significant preference for addition by the same trajectory that leads to hydrolysis of the matched enantiomer of epoxide, with a selectivity that is nearly identical to the observed stereoselectivity in the HKR of terminal epoxides. This provides a most compelling, final piece of evidence that stereoselectivity arises from the relative orientation of the two (salen)Co(III) catalysts and not from specific interactions of the chiral epoxide enantiomers with the chiral catalysts.

CONCLUSIONS

A range of experimental and computational data support the proposal that the asymmetric induction in the epoxide ring-opening step of the HKR is controlled by interactions between

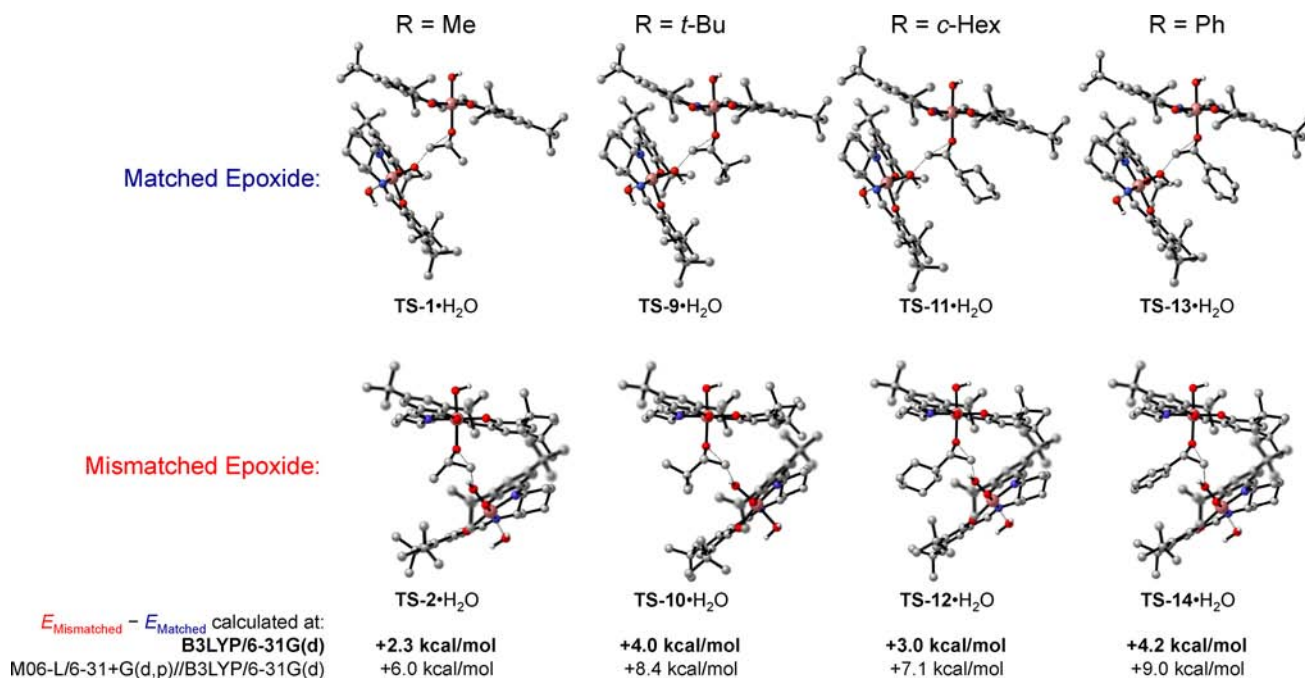


Figure 17. Effect of the epoxide substituent on calculated stereoselectivity. Epoxide ring-opening transition structures optimized at the B3LYP/6-31G(d) level of theory are presented along with the difference in energy between the “matched” and “mismatched” transition structures. C–H bonds are omitted for clarity.

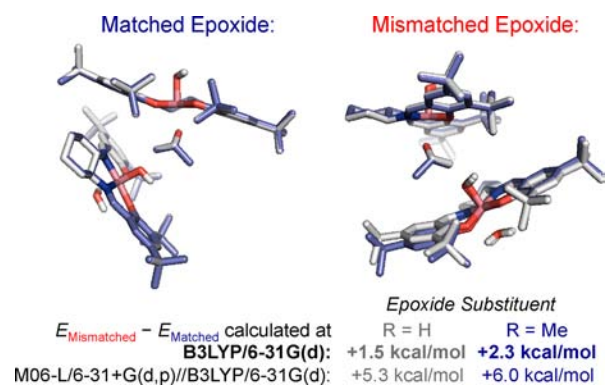


Figure 18. Computed selectivity for the hypothetical epoxide ring-opening reaction of ethylene oxide. The epoxide methyl substituent in TS-1·H₂O and TS-2·H₂O was replaced with a hydrogen atom, and the resulting structure was optimized to a transition structure at the B3LYP/6-31G(d) level. The resulting structures were overlaid with their parent structures by minimizing the root-mean-square deviation between the six atoms in the Lewis acidic Co(III) center’s coordination sphere. C–H bonds are omitted for clarity.

two (salen)Co(III) complexes and that these interactions are mediated by the chiral, stepped conformations of the salen ligand. Furthermore, and perhaps more significantly, this model does not require a steric clash with the epoxide substituent to achieve stereoselectivity, providing an explanation for the extraordinary breadth of the HKR’s substrate scope. Key findings include the following:

(1) Kinetic analyses using mixtures of (*R,R*)-, (*S,S*)-, and/or *meso*-(salen)Co(III) complexes establish that the absolute stereochemistry of Lewis acidic and nucleophilic catalysts must be matched to the chiral epoxide for any measurable hydrolysis to occur, and that the chiral, stepped conformation of the salen ligand mediates this stereochemical match.

(2) Computational studies show that epoxides bind to the cobalt center in almost identical geometries, that this geometry is insensitive to epoxide substituent and stereochemistry, and that there is a significant energetic penalty for accessing other binding orientations. DFT calculations also support the conclusion drawn from previous kinetic studies that the hexacoordinate singlet **1b**·H₂O is a competent nucleophile in epoxide-opening chemistry.

(3) A computational analysis of bimetallic ring-opening transition structures with the full catalyst structure reproduces the matched stereochemical relationship between the catalysts and the epoxide that is observed experimentally. These transition structures led to the identification of a catalyst–catalyst interaction that may be important for selectivity, and this proposal was validated by demonstrating experimentally that stereoselectivity is highly sensitive to the steric demands of substituents on the salen aromatic ring that are distant from the cobalt center.

(4) Computational investigations of hypothetical mono-metallic epoxide ring-opening reactions show that neither the Lewis acidic nor the nucleophile-delivering (salen)Co(III) complex is able to achieve stereoselectivity on its own, and selectivity is only achieved in the bimetallic assembly. This supports the conclusion that stereochemical communication between catalysts is key to selectivity.

(5) Finally, inspection of the calculated transition structures led us to the observation that the epoxide substituent—which can be changed to nearly any organic fragment without the selectivity factor dropping below 50—projects into open space. Indeed, the spatial relationship between the two (salen)Co(III) catalysts in the epoxide ring-opening transition structure changed very little when we replaced our model epoxide, propylene oxide, with other epoxides with larger substituents or with no substituent at all (ethylene oxide), indicating that a steric interaction between the epoxide substituent and the catalyst is not required for high stereoselectivity. We conclude

that the role of the epoxide substituent is simply to position the epoxide's less-substituted electrophilic reactive site with respect to the catalyst. This serves to explain how enantiomeric epoxides can be resolved efficiently without relying on a specific interaction with the epoxide substituent.

More broadly, the mechanistic model for the HKR developed here provides a rationalization for how the HKR can be both so highly stereoselective and broad in scope with respect to terminal epoxide substrates. All terminal epoxides bind in essentially the same geometry and are subject to the same interactions with the catalyst in the ground state and the transition state. Binding of the epoxide ring in a specific orientation reduces the problem of selectively opening one enantiomer of a broad range of epoxides to the more straightforward proposition of discriminating between two trajectories along which two chiral (salen)Co(III) complexes can react. Hence, selectivity is primarily controlled by interactions between the aromatic groups of the two salen ligands, which are expected to be quite similar with different nucleophile–electrophile combinations. It seems likely that the lessons gleaned from this work will be valuable in helping to elucidate the basis for high stereoselectivity in other reactions in which two metal–salen complexes operate cooperatively, as has been documented or implicated in asymmetric epoxide ring-opening reactions with other nucleophiles,^{4,7,55} ring-opening of oxetanes,⁵⁶ (salen)Al(III)-catalyzed conjugate addition reactions,⁵⁷ stereoselective epoxide polymerization,⁵⁸ and epoxide/CO₂ copolymerization.⁵⁹

This work joins a growing body of research that has been directed toward elucidating the mechanisms of so-called “privileged” chiral catalysts.⁶⁰ While the immediate practical goal of such mechanistic investigation may be to improve and expand these particular catalyst systems, a broader, more fundamental objective is to understand how small-molecule chiral catalysts such as metal–salen complexes can be so effective in catalyzing a wide variety of enantioselective transformations with broad substrate scope. It is hoped that detailed mechanistic investigations such as the one described here may help guide the discovery of new classes of broadly useful asymmetric catalysis methods in the future.

■ ASSOCIATED CONTENT

● Supporting Information

Experimental procedures, ¹H and ¹³C NMR spectra of ligands and complexes, kinetic data in tabular format, and Cartesian coordinates of computed complexes. This material is available free of charge via the Internet at <http://pubs.acs.org>.

■ AUTHOR INFORMATION

Corresponding Author

jacobsen@chemistry.harvard.edu

Notes

The authors declare no competing financial interest.

■ ACKNOWLEDGMENTS

We thank Dr. Robert R. Knowles, Prof. Theodore A. Betley, and Dr. Eugene E. Kwan for helpful discussions. This work was supported by the NIH (GM-43214) and by fellowship support to D.D.F. from Eli Lilly and Co. and to L.P.C.N. from the Hertz Foundation.

■ REFERENCES

- (1) (a) Tokunaga, M.; Larrow, J. F.; Kakiuchi, F.; Jacobsen, E. N. *Science* **1997**, *277*, 936–938. (b) Schaus, S. E.; Brandes, B. D.; Larrow, J. F.; Tokunaga, M.; Hansen, K. B.; Gould, A. E.; Furrow, M. E.; Jacobsen, E. N. *J. Am. Chem. Soc.* **2002**, *124*, 1307–1315. (c) Stevenson, C. P.; Nielsen, L. P. C.; Jacobsen, E. N.; McKinley, J. D.; White, T. D.; Couturier, M. A.; Ragan, J. *Org. Synth.* **2006**, *83*, 162–169.
- (2) For reviews of applications of the HKR reaction in industrial and natural products synthesis, see: (a) Larrow, J. F.; Hemberger, K. E.; Jasmin, S.; Kabir, H.; Morel, P. *Tetrahedron: Asymmetry* **2003**, *14*, 3589–3592. (b) Schneider, C. *Synthesis* **2006**, 3919–3944. (c) Kumar, P.; Naidu, V.; Gupta, P. *Tetrahedron* **2007**, *63*, 2745–2785. (d) Furukawa, Y.; Suzuki, T.; Mikami, M.; Kitaori, K.; Yoshimoto, H. *J. Synth. Org. Chem. Jpn.* **2007**, *65*, 308–319. (e) Kumar, P.; Gupta, P. *Synlett* **2009**, 1367–1382. (f) Pellissier, H. *Adv. Synth. Catal.* **2011**, *353*, 1613–1666.
- (3) Throughout this paper, we will refer to the property of the HKR catalysts to differentiate between substrate enantiomers as “stereoselectivity”. Stereoselectivity in any kinetic resolution is most unambiguously defined by the relative rate of reaction with the two enantiomers of the substrate (k_{rel}). We choose this term instead of “enantioselectivity”, which is applied more commonly to describe chiral catalysts, but generally refers to the enantiomer ratio (er) or enantiomeric excess (ee) obtained from an achiral or rapidly racemizing substrate.
- (4) (salen)Cr(III): Hansen, K. B.; Leighton, J. L.; Jacobsen, E. N. *J. Am. Chem. Soc.* **1996**, *118*, 10924–10925.
- (5) Jacobsen, E. N. *Acc. Chem. Res.* **2000**, *33*, 421–431.
- (6) (a) Nielsen, L. P. C.; Stevenson, C. P.; Blackmond, D. G.; Jacobsen, E. N. *J. Am. Chem. Soc.* **2004**, *126*, 1360–1362. (b) Nielsen, L. P. C.; Zuend, S. J.; Ford, D. D.; Jacobsen, E. N. *J. Org. Chem.* **2012**, *77*, 2486–2495.
- (7) Ready, J. M.; Jacobsen, E. N. *J. Am. Chem. Soc.* **2001**, *123*, 2687–2688.
- (8) (a) Jain, S.; Zheng, X.; Jones, C. W.; Weck, M.; Davis, R. J. *Inorg. Chem.* **2007**, *46*, 8887–8896. (b) Jain, S.; Venkatasubbaiah, K.; Jones, C. W.; Davis, R. J. *J. Mol. Catal. A: Chem.* **2010**, *316*, 8–15.
- (9) Selected reviews of other cooperative catalysis schemes—Synergistic catalysis: (a) Allen, A. E.; MacMillan, D. W. C. *Chem. Sci.* **2012**, *3*, 633–658. Bifunctional/multifunctional catalysis: (b) Breslow, R. *J. Mol. Catal.* **1994**, *91*, 161–174. (c) Shibasaki, M.; Yoshikawa, N. *Chem. Rev.* **2002**, *102*, 2187–2209. (d) Paull, D. H.; Abraham, C. J.; Scerba, M. T.; Alden-Danforth, E.; Lectka, T. *Acc. Chem. Res.* **2008**, *41*, 655–663. (e) Shibasaki, M.; Kanai, M.; Matsunaga, S.; Kumagai, N. *Acc. Chem. Res.* **2009**, *42*, 1117–1127. Metal–organic cooperative catalysis: (f) Park, Y. J.; Park, J.-W.; Jun, C.-H. *Acc. Chem. Res.* **2008**, *41*, 222–234. The HKR and other related (salen)metal-catalyzed asymmetric ring-opening reactions stand apart from the above categories of cooperative catalysis because one catalyst serves to activate each reaction partner individually, and these activated species then react with one another in a bimetallic ring-opening step.
- (10) For a recently reported effort at addressing this question, see: Key, R. E.; Venkatasubbaiah, K.; Jones, C. W. *J. Mol. Catal. A: Chem.* **2013**, *366*, 1–7.
- (11) (a) Girard, C.; Kagan, H. B. *Angew. Chem., Int. Ed.* **1998**, *37*, 2922–2959. (b) Satyanarayana, T.; Abraham, S.; Kagan, H. B. *Angew. Chem., Int. Ed.* **2009**, *48*, 456–494.
- (12) (a) Ismagilov, R. F. *J. Org. Chem.* **1998**, *63*, 3772–3774. (b) Luukas, T. O.; Girard, C.; Fenwick, D. R.; Kagan, H. B. *J. Am. Chem. Soc.* **1999**, *121*, 9299–9306. (c) Blackmond, D. G. *J. Am. Chem. Soc.* **2001**, *123*, 545–553.
- (13) Johnson, D. W., Jr.; Singleton, D. A. *J. Am. Chem. Soc.* **1999**, *121*, 9307–9312.
- (14) This conclusion receives further validation from computational analyses described later in this paper (sections 6 and 7).
- (15) Larrow, J. F.; Jacobsen, E. N. *Top. Organomet. Chem.* **2004**, *6*, 123–152.

(16) (a) Initial report and analysis of stereoreduction: Jacobsen, E. N.; Zhang, W.; Muci, A. R.; Ecker, J. R.; Deng, L. *J. Am. Chem. Soc.* **1991**, *113*, 7063–7064. (b) For a comprehensive review, see: McGarrigle, E. M.; Gilheany, D. G. *Chem. Rev.* **2005**, *105*, 1563–1602.

(17) Yoon, T. P.; Jacobsen, E. N. *Science* **2003**, *299*, 1691–1693.

(18) For discussions of the step-like conformation of (salen)Mn(V)-oxo complexes, see: (a) Cavallo, L.; Jacobsen, H. *Chem.—Eur. J.* **2001**, *7*, 800–807. (b) Katsuki, T. *Adv. Synth. Catal.* **2002**, *344*, 131–147. (c) El-Bahraoui, J.; Wiest, O.; Feichtinger, D.; Plattner, D. A. *Angew. Chem., Int. Ed.* **2001**, *40*, 2073–2076. (d) Cavallo, L.; Jacobsen, H. *J. Org. Chem.* **2003**, *68*, 6202–6207. For the crystal structure of an achiral, stepped (salen)Cr(V)-oxo complex, see: (e) Samsel, E. G.; Srinivasan, K.; Kochi, J. K. *J. Am. Chem. Soc.* **1985**, *107*, 7606–7617.

(19) In contrast, little deviation from planarity is observed in crystal structures of (salen)Mn(III) complexes: Pospisil, P. J.; Carsten, D. H.; Jacobsen, E. N. *Chem.—Eur. J.* **1996**, *2*, 974–980.

(20) Bobb, R.; Alkahimi, G.; Studnicki, L.; Lough, A.; Chin, J. *J. Am. Chem. Soc.* **2002**, *124*, 4544–4545.

(21) (a) Zhang, F.; Bai, S.; Yap, G. P. A.; Tarwade, V.; Fox, J. M. *J. Am. Chem. Soc.* **2005**, *127*, 10590–10599. (b) Dong, Z.; Karpowicz, R. J., Jr.; Bai, S.; Yap, G. P. A.; Fox, J. M. *J. Am. Chem. Soc.* **2006**, *128*, 14242–14243. (c) Dong, Z.; Yap, G. P. A.; Fox, J. M. *J. Am. Chem. Soc.* **2007**, *129*, 11850–11853. (d) Fisher, L. A.; Zhang, F.; Yap, G. P. A.; Fox, J. M. *Inorg. Chim. Acta* **2010**, *364*, 259–260. (e) Dong, Z.; Plampin, J. N., III; Yap, G. P. A.; Fox, J. M. *Org. Lett.* **2010**, *12*, 4002–4005. (f) Dong, Z.; Bai, S.; Yap, G. P. A.; Fox, J. M. *Chem. Commun.* **2011**, *47*, 3781–3783.

(22) In a series of elegant studies, Fox and co-workers have shown that the match between the sense of helical chirality in a metal–salen complex and the absolute stereochemistry of the diamine backbone can be overturned in the context of (salen)Ni(II) metallofoldamers by introducing stereogenic end-groups at the salicylidene 3-position (ref 21). While Fox's work raises the possibility that a similar phenomenon might occur in (salen)Co(III) structures, i.e., that diastereomeric complexes (*P,S,S*)- and (*M,S,S*)-**1b** could both be present in HKR reaction mixtures, an examination of the crystal structures of the (salen)Ni(II)-derived metallofoldamers reveals a conformation of the salen ligand that is distinct from that of the (salen)Co(III) step structures that are the focus here. In the (salen)Ni(II) structures, the ligand appears to be twisted out of planarity into a helix, as opposed to adopting the salen step. Indeed, a crystal structure of (salen)Ni(II) complexes with the same ligand as in complexes **1** reveals no salen step; instead, the ligand takes on a slight twist (see: Shimazaki, Y.; Tani, F.; Fukui, K.; Naruta, Y.; Yamauchi, O. *J. Am. Chem. Soc.* **2003**, *125*, 10512–10513). For the purpose of our analysis of (salen)Co(III) complexes, we make the assumption that there is only a single energetically accessible diastereomer of **1b**, with the step absolute stereochemistry matched to the diamine absolute stereochemistry.

(23) (a) Hashihayata, T.; Ito, Y.; Katsuki, T. *Synlett* **1996**, 1079–1081. (b) Hashihayata, T.; Ito, Y.; Katsuki, T. *Tetrahedron* **1997**, *53*, 9541–9552. (c) Miura, K.; Katsuki, T. *Synlett* **1999**, 783–785. (d) Liao, S.; List, B. *Angew. Chem., Int. Ed.* **2010**, *49*, 628–631.

(24) In the recently discovered (salen)Co(III)-catalyzed epoxide fluorination reaction, there is a strong matched/mismatched relationship between the absolute stereochemistry of a chiral amine additive and the absolute stereochemistry of the salen ligand. In addition, modest levels of selectivity can be achieved using ethylene diamine-derived (salen)Co-OTs catalyst **2d** in conjunction with these chiral additives. These effects may be attributed to the chiral additive serving as an axial ligand on the (salen)Co(III) complex, thereby favoring one chiral salen step conformer over the other, but the complexity of the mechanism of these reactions would make it difficult to determine the precise stereochemical role of the chiral additive. (a) Kalow, J. A.; Doyle, A. G. *J. Am. Chem. Soc.* **2010**, *132*, 3268–3269. (b) Kalow, J. A.; Doyle, A. G. *J. Am. Chem. Soc.* **2011**, *133*, 16001–16012.

(25) van den Bergen, A. M.; Fallon, G. D.; West, B. O. Cambridge Crystallographic Database, deposition no. CCDC 136763, 1999.

(26) For crystal structures of cationic (salen)Co(III) complexes possessing only L-type axial ligands, see: (a) Bobb, R.; Alkahimi, G.;

Studnicki, L.; Lough, A.; Chin, J. *J. Am. Chem. Soc.* **2002**, *124*, 4544–4545. (b) Huang, Y.; Iwama, T.; Rawal, V. H. *J. Am. Chem. Soc.* **2002**, *124*, 5950–5951. (c) Hutson, G. E.; Dave, A. H.; Rawal, V. H. *Org. Lett.* **2007**, *9*, 3869–3872.

(27) For crystal structures of neutral (salen)Co(III) complexes possessing an X-type axial ligand, see: (a) Ready, J. M.; Jacobsen, E. N. *J. Am. Chem. Soc.* **2001**, *123*, 2687–2688. (b) Hong, J. Ph.D. Thesis, Harvard University, Cambridge, MA, October 2001. (c) Cohen, C. T.; Thomas, C. T.; Peretti, K. L.; Lobkovsky, E. B.; Coates, G. W. *Dalton Trans.* **2006**, 237–249.

(28) For a compilation of crystal structures of (salen)metal complexes, see: Nielsen, L. P. C. Ph.D. Thesis, Harvard University, Cambridge, MA, November 2006; Appendix 1. The complete text of this document is available via the Internet through Proquest (<http://www.proquest.com>).

(29) The achiral (salen)Co(III) complexes in Figure 7 exist in chiral conformations that may or may not undergo racemization rapidly on the time scale of the epoxide hydrolysis reactions. For the purposes of this analysis, the only important issue is that they exist as 50:50 mixtures of the stepped, chiral conformers.

(30) The small rate difference between **1b** and **3b** (at double the concentration) was reproduced with several different batches of catalysts. It can be ascribed to several factors, including the fact that the step conformations are similar but not identical in the two catalysts (Figure 7) and/or that the concentrations of (*P*)-**3b** and (*M*)-**3b** are not necessarily identical in the presence of the chiral epoxide.

(31) The “0.5 mol% **3b**” and “0.5 mol% **3b** + 0.2 mol% (*R,R*)-**1b**” curves are not perfectly superimposable. Although this effect is small (<10% difference in rate), it is reproducible.

(32) (a) Becke, A. D. *Phys. Rev. A* **1988**, *38*, 3098–3100. (b) Lee, C.; Yang, W.; Parr, R. G. *Phys. Rev. B* **1988**, *37*, 785–789. (c) Becke, A. D. *J. Chem. Phys.* **1993**, *98*, 1372–1377. (d) Stephens, P. J.; Devlin, F. J.; Chabalowski, C. F.; Frisch, M. J. *J. Phys. Chem.* **1994**, *98*, 11623–11627.

(33) Selected examples of the application of B3LYP in quantum chemical calculations of transition metal structure and reactivity: (a) Strassner, T.; Taige, M. A. *J. Chem. Theory Comput.* **2005**, *1*, 848–855. (b) Jenkins, D. M.; Di Bilio, A. J.; Allen, M. J.; Betley, T. A.; Peters, J. C. *J. Am. Chem. Soc.* **2002**, *124*, 15336–15350. (c) Takaoka, A.; Peters, J. C. *Inorg. Chem.* **2012**, *51*, 16–18. (d) Shakya, R.; Imbert, C.; Hratchian, H. P.; Lanznaster, M.; Heeg, M. J.; McGarvey, B. R.; Allard, M.; Schlegel, B.; Verani, C. N. *Dalton Trans.* **2006**, 2517–2525. (e) Araujo, C. M.; Doherty, M. D.; Konezny, S. J.; Luca, O. R.; Ustyatinsky, A.; Grade, H.; Lobkovsky, E.; Soloveichik, G. L.; Crabtree, R. H.; Batista, V. S. *Dalton Trans.* **2012**, *41*, 3562–3573. (f) Wang, T.; Brudvig, G.; Batista, V. S. *J. Chem. Theory Comput.* **2010**, *6*, 755–760.

(34) Selected examples of studies documenting the drawbacks of B3LYP: Zhao, Y.; Truhlar, D. G. *J. Chem. Phys.* **2006**, *124*, 224105. See also ref 44.

(35) We performed calculations with B3LYP, OLYP, TPSSh, BP86, PW91, and M06L, using basis sets as large as 6/311+G(d,p) and ccPVTZ.

(36) As would be expected for a six-coordinate d^6 Co(III) complex, the **1b**-epoxide complexes are all most stable as closed-shell singlets. A more detailed discussion of spin state in (salen)Co(III) complexes can be found in the next section.

(37) Nearly identical binding geometries are observed in two crystal structures of *cis*-disubstituted aziridines bound to cationic (salen)Co(III) complexes, with $\theta = 40$ – 52° (Figure 4 and ref 17). These values represent a range of six values of θ culled from two crystal structures. Each cationic (salen)Co(III) unit has two bound aziridines, and in one of the crystal structures, there are two crystallographically distinct (salen)Co(III) units. The similarities in the binding geometries of epoxides and aziridines to (salen)Co(III) are striking given the different electronic and steric properties of these ligands.

(38) Kemper, S.; Hrobárik, P.; Kaupp, M.; Schlörer, N. E. *J. Am. Chem. Soc.* **2009**, *131*, 4172–4173.

(39) For the purposes of this discussion, compound numbers are labeled with their spin multiplicity. For example, $^{2S+1}\mathbf{1}$ refers to an

electronic configuration of compound **1** with a total spin quantum number of S .

(40) Sutton, P. A.; Buckingham, D. A. *Acc. Chem. Res.* **1987**, *20*, 357–364.

(41) The kinetic non-lability of six-coordinate Co(III) complexes is well established: (a) Crabtree, R. H. *The Organometallic Chemistry of the Transition Metals*, 4th ed.; John Wiley & Sons: Hoboken, NJ, 2005; pp 11–12. (b) The effect is illustrated in a dramatic way by the fact that hexaaminecobalt(III) chloride can be purified by recrystallization from concentrated hydrochloric acid in high yield: Bjerrum, J.; McReynolds, J. P. *Inorg. Synth.* **1946**, *2*, 216–221.

(42) In both five- and six-coordinate complexes, the quintet ($S = 2$) spin state was higher in energy (see Supporting Information), and it was not considered further.

(43) We also considered the valence tautomer of **31b**, in which cobalt is in the +II oxidation state ($S_{Co} = 3/2$) and the salen ligand is oxidized by one electron and is antiferromagnetically coupled to the metal center ($S_{salen} = -1/2$), but these species do not appear to be stable: no structures of this type were located. Nevertheless, as others have observed, the computed structure of **31b** appears to have a resonance contribution from a Co(II)–phenoxy representation. Spin density maps and molecular orbitals relevant to our analysis are presented in the Supporting Information. A detailed analysis of cationic (salen)Co(OH₂)⁺ yielded EPR and magnetic susceptibility data that support significant Co(II)–phenoxy character: (a) Kochem, A.; Kanso, H.; Baptiste, B.; Arora, H.; Philouze, C.; Jarjays, O.; Vezin, H.; Luneau, D.; Orio, M.; Thomas, F. *Inorg. Chem.* **2012**, *51*, 10557–10571. In contrast, further one-electron oxidation of (salen)Co(III) complexes occurs on the ligand to generate the Co(III)–phenoxy. For a detailed discussion of ligand-centered redox behavior in (salen)Co complexes, see: (b) Vinck, E.; Murphy, D. M.; Fallis, I. A.; Strevens, R. R.; Van Doorslaer, S. *Inorg. Chem.* **2010**, *49*, 2083–2092. For examples with other, related complexes, see: (c) Ray, K.; Begum, A.; Weyhermüller, T.; Piligkos, S.; van Slageren, J.; Neese, F.; Wieghardt, K. *J. Am. Chem. Soc.* **2005**, *127*, 4403–4415. (d) Smith, A. L.; Hardcastle, K. I.; Soper, J. D. *J. Am. Chem. Soc.* **2010**, *132*, 14358–14360.

(44) Key calculations were repeated using other exchange functionals that have been used to reproduce spin state preferences for Co(III) complexes correctly. For evaluations of DFT performance with Co(III) spin state ordering, see: (a) Wasbotten, I. H.; Ghosh, A. *Inorg. Chem.* **2007**, *46*, 7890–7896. (b) Takatani, T.; Sears, J. S.; Sherrill, C. D. *J. Phys. Chem. A* **2009**, *113*, 9231–9236. (c) Jensen, K. P.; Cirera, J. *J. Phys. Chem. A* **2009**, *113*, 10033–10039. (d) Ghosh, A. *J. Biol. Inorg. Chem.* **2006**, *11*, 712–724.

(45) The data presented in Figure 14 show that the epoxide ring-opening step has a higher activation barrier, but is considerably more favorable thermodynamically when the (salen)Co–OH complex undergoes reaction from the triplet spin state instead of the singlet spin state. Calculations repeated with implicit solvent modeling show that this difference in energy is predominantly an artifact of the penalty for charge separation in the gas phase: whereas precomplex **3SM-1** and transition structure **3TS-1** have unpaired spin density localized to the nucleophile-delivering (salen)Co(III) complex, the bimetallic product of reaction from the triplet manifold is predicted computationally to undergo disproportionation to a Co(II)/Co(IV) complex to minimize this charge separation. This behavior is not observed when solvation models are applied. However, this effect becomes significant only after the rate- and selectivity-determining transition structure. Accordingly, we opted to conduct the remainder of our analyses using gas-phase calculations, which were found to converge more rapidly and consistently than calculations carried out with solvent correction. See the Supporting Information for additional details.

(46) We are mindful not to draw too strong of a conclusion from an energy difference of this magnitude involving structures of two different spin states, especially with a fairly basic DFT method. The important conclusion is that the hydroxo ligand can react as a nucleophile with an activated epoxide without dissociating from the Co(III) center and that the barrier to this reaction is comparable to the hydroxo in **31b**. A survey of other computational methods reveals that

some functionals predict **31b** to be slightly more nucleophilic than **1b**–H₂O, making it difficult to draw a conclusion about the absolute nucleophilicities of these hydroxo complexes (see the Supporting Information). Nonetheless, the computational models all show that **1b**–H₂O is both stable and highly nucleophilic.

(47) Zhao, Y.; Truhlar, D. G. *Theor. Chem. Acc.* **2008**, *120*, 215–241.

(48) (a) Zuend, S. J.; Jacobsen, E. N. *J. Am. Chem. Soc.* **2009**, *131*, 15358–15374. (b) Uyeda, C.; Jacobsen, E. N. *J. Am. Chem. Soc.* **2011**, *133*, 5062–5075.

(49) For examples of electronic or steric tuning of chiral (salen)metal complexes by variation of the salicylidene 5-substituent, see: (a) Palucki, M.; Finney, N. S.; Pospisil, P. J.; Guler, M. L.; Ishida, T.; Jacobsen, E. N. *J. Am. Chem. Soc.* **1998**, *120*, 948–955. (b) Doyle, A. G.; Jacobsen, E. N. *Angew. Chem., Int. Ed.* **2007**, *46*, 3701–3705.

(50) Kinetic analyses with some of these catalysts also reveal an approximately second-order dependence on catalyst loading, suggesting that these catalysts promote hydrolysis via a cooperative, bimetallic mechanism. In this analysis, we have also found that catalysts that induce higher enantioselectivity are also generally more reactive. Although the basis for this rate acceleration effect is not known, it is possible that different degrees of solvation of the largely hydrophobic catalyst in a hydrophilic reaction mixture may play a role.

(51) The enantioselectivity trends determined by GC analysis are reproduced well by reaction calorimetry experiments in which the rates of hydrolysis of (R)- and (S)-1,2-epoxyhexane were measured independently. See the Supporting Information for details.

(52) The measured selectivity factor for R = *t*-Bu is larger than the selectivity factor obtained previously from analogous experiments. Measuring selectivity factors of this magnitude is technically challenging. For a discussion of the factors that might limit accuracy and precision in the determination of selectivity factors in the HKR, see ref 1b. The experimental procedure used for the determination of selectivity factors is included in the Supporting Information.

(53) The data also suggest there is a leveling effect with very large substituents, and substituents larger than *tert*-butyl appear to induce slightly lower enantioselectivity (i.e., R = trimethylsilyl induces lower enantioselectivity than R = *t*-Bu). Preliminary calorimetry experiments using (salen)Co–Cl complexes with substituents larger than trimethylsilyl (i.e., triethylsilyl and tripropylsilyl) indicate that this trend continues.

(54) We note that while the selectivities predicted for these epoxides do not follow the experimental trends—*tert*-butyl and phenyl substituents lead to lower selectivities than cyclohexyl or methyl^{1b}—these epoxide are all excellent substrates for the HKR, and our calculations predict high selectivities for each of them. It seems likely that differences in selectivity between these epoxides are driven by weak dispersion interactions, which B3LYP is not well suited to accurately reproduce.

(55) (a) Bartoli, G.; Bosco, M.; Carlone, A.; Locatelli, M.; Melchiorre, P.; Sambri, L. *Org. Lett.* **2004**, *6*, 3973–3975. (b) Bartoli, G.; Bosco, M.; Carlone, A.; Locatelli, M.; Melchiorre, P.; Sambri, L. *Org. Lett.* **2005**, *7*, 1983–1985. (c) Birrell, J. A.; Jacobsen, E. N. *Org. Lett.* **2013**, *15*, 2895–2897.

(56) Loy, R. N.; Jacobsen, E. N. *J. Am. Chem. Soc.* **2009**, *131*, 2786–2787.

(57) Mazet, C.; Jacobsen, E. N. *Angew. Chem., Int. Ed.* **2008**, *47*, 1762–1765.

(58) (a) Peretti, K. L.; Ajiro, H.; Cohen, C. T.; Lobkovsky, E. B.; Coates, G. W. *J. Am. Chem. Soc.* **2005**, *127*, 11566–11567. (b) Thomas, R. M.; Widger, P. C. B.; Ahmed, S. M.; Jeske, R. C.; Hirahata, W.; Lobkovsky, E. B.; Coates, G. W. *J. Am. Chem. Soc.* **2010**, *132*, 16520–16525.

(59) Cohen, C. T.; Thomas, C. M.; Peretti, K. L.; Lobkovsky, E. B.; Coates, G. W. *Dalton Trans.* **2006**, 237–249.

(60) *Privileged Chiral Ligands and Catalysts*; Zhou, Q.-L., Ed.; Wiley-VCH: Weinheim, Germany, 2011.